Ann Surg Oncol (2019) 26:4537–4547
https://doi.org/10.1245/s10434-019-07815-9

Annals of
SURGICAL ONCOLOGY
OFFICIAL JOURNAL OF THE SOCIETY OF SURGICAL ONCOLOGY

ORIGINAL ARTICLE – HEPATOBILIARY TUMORS

Preoperative Radiomic Approach to Evaluate Tumor-Infiltrating CD8$^+$ T Cells in Hepatocellular Carcinoma Patients Using Contrast-Enhanced Computed Tomography

Haotian Liao, MD[1,4], Zhen Zhang, MD[2], Jie Chen, MD[2], Mingheng Liao, MD, PhD[1,4], Lin Xu, MD[1,4], Zhenru Wu, MD[3], Kefei Yuan, PhD[1,4], Bin Song, MD, PhD[2], and Yong Zeng, MD, PhD[1,4]

[1]Department of Liver Surgery, Liver Transplantation Division, West China Hospital, Sichuan University, Chengdu, Sichuan, People's Republic of China; [2]Department of Radiology, West China Hospital, Sichuan University, Chengdu, Sichuan, People's Republic of China; [3]Laboratory of Pathology, Department of Pathology, West China Hospital, Sichuan University, Chengdu, Sichuan, People's Republic of China; [4]Laboratory of Liver Surgery, West China Hospital, Sichuan University, Chengdu, Sichuan, People's Republic of China

ABSTRACT

Background. To help identify potential hepatocellular carcinoma (HCC) candidates for immunotherapies, we aimed to develop and validate a radiomics-based biomarker (Rad score) to predict the infiltration of tumor-infiltrating CD8$^+$ T cells in HCC patients, and to evaluate the correlation of Rad score with tumor immune characteristics.

Methods. Overall, 142 HCC patients (n = 100 and n = 42 in the training and validation sets, respectively) were subjected to radiomic feature extraction. Imaging features and immunochemistry data of patients in the training set were subjected to elastic-net regularized regression analysis to predict the level of CD8$^+$ T cell infiltration.

Results. A Rad score for CD8$^+$ T-cell infiltration, which contained seven variables, was developed and was validated in the validation set (area under the curve [AUC]: training set 0.751, 95% confidence interval [CI] 0.656–0.846; validation set 0.705, 95% CI 0.547–0.863). The decision curve indicated the clinical usefulness of the Rad score. A higher Rad score correlated with superior overall and disease-free survival outcomes (p = 0.012 and 0.0088, respectively). Using the pathological slides, we found that the Rad score positively correlated with the percentage of tumor-infiltrating lymphocytes (TILs; Spearman rho = 0.51, $p < 0.0001$). Moreover, the Rad score could also discriminate inflamed tumors from immune-desert and immune-excluded tumors (Kruskal–Wallis, $p < 0.0001$), and higher Rad scores could be found in patients with positive programmed cell death ligand 1 expression in tumor/immune cells, as well as those with positive programmed cell death protein 1 expression.

Conclusion. The newly developed Rad score was a powerful predictor of CD8$^+$ T-cell infiltration, which could be useful in identifying potential HCC patients who can benefit from immunotherapies when validated in large-scale prospective cohorts.

With over 400,000 newly diagnosed cases and deaths in 2015, hepatocellular carcinoma (HCC) has become one of the most common malignancies in China.[1] Conventionally, the management of HCC is evolving dramatically with the expansion of resection criteria, improved locoregional therapies, advent of novel targeted systemic therapies, newer techniques for internal and external radiation therapy, and the possibility of transplantation.[2] Despite great

Haotian Liao and Zhen Zhang contributed equally to this work.

Electronic supplementary material The online version of this article (https://doi.org/10.1245/s10434-019-07815-9) contains supplementary material, which is available to authorized users.

First Received: 13 May 2019;
Published Online: 13 September 2019

B. Song, MD, PhD
e-mail: songb_radiology@163.com

Y. Zeng, MD, PhD
e-mail: zengyong@medmail.com.cn

advances achieved in the treatment of HCC, patients are still suffering from poor prognosis.[3] Thus, it is highly desirable to expand the therapeutic arsenal for HCC.

Recently, the development of immunotherapy has substantially changed the therapeutic strategies for various cancers, including melanomas, lymphomas, and lung tumors.[4–6] For HCC patients, a small phase II trial targeting patients with HCC and chronic hepatitis C virus infection tested an anti-CTLA-4 monoclonal antibody, tremelimumab, and showed a notable disease control rate.[7] Moreover, in September 2017, the US FDA granted accelerated approval to the anti-programmed cell death protein 1 (PD-1) monoclonal antibody nivolumab for the treatment of HCC patients who have been previously treated with sorafenib. These facts suggest the future promotion of immunotherapy on HCC. However, only a small portion of HCC patients receiving nivolumab treatment responded to the therapy;[8] therefore, there is an urgent need to find efficient methods to identify HCC patients who are most likely to respond to immunotherapies. Previous studies have reported that patient response to anti-PD-1 and anti-programmed cell death ligand 1 (PD-L1) immunotherapy was correlated with pre-existing tumoral and peritumoral immune infiltration, indicating the density of immune infiltration may provide evidence for predicting prognosis after anti-PD-1 or anti-PD-L1 treatment.[9–12]

Computational medical imaging, known as radiomics, refers to the high-throughput extraction of large numbers of imaging features, and can convert medical images into mineable high-dimensional data, of which analysis and translation can help support decision making for patient treatment.[13–15] Based on the hypothesis that not only the macroscopic properties but also the cellular and molecular properties of tumor tissues can be reflected by imaging, high-dimensional imaging data can capture distinct phenotypic differences of tumors, which may have prognostic power and clinical significance.[16] Compared with biopsies, radiomic features have the advantage of being non-invasive, which allows evaluation on tumor microenvironment (TME), characterization of spatial heterogeneity, and longitudinal assessment of disease evolution.

Hence, in this study, we sought to develop and validate a radiomic signature of immune infiltration in HCC by using radiomic data extracted from contrast-enhanced computed tomography (CT) images, which can help us identify the novel predictors for the efficacy of immunotherapy.

METHODS

Study Population

This retrospective study was approved by the Ethics Committee of Sichuan University, and written informed consent was obtained from each study participant according to the committee guidelines. A total of 142 consecutive patients with HCC who were treated between July 2009 and September 2013 were enrolled in our study according to the following inclusion criteria: (1) patients undergoing hepatectomy with tumor tissues pathologically confirmed as HCC; (2) contrast-enhanced abdominal CT performed fewer than 20 days before surgery; and (3) availability of clinical data and tumor samples. The exclusion criteria were (1) previous treatment before CT examination; and (2) suffering from other tumor diseases at the same time. The flowchart of patient recruitment is illustrated in electronic supplementary Fig. 1. Patients were divided into the training (n = 100) and validation cohorts (n = 42) at a ratio of 7:3 according to the time sequence.

Recorded clinical and biological data, including age, sex, hepatitis B surface antigen (HBsAg) status (positive or negative), and preoperative serum α-fetoprotein (AFP) level, were retrieved from the electronic medical database. The characteristics of tumor samples, including differentiation status, size, number of nodules, and Ishak fibrosis score of the adjacent liver tissue were evaluated by two pathologists specializing in hepatic diseases. Tumor staging classification was carried out according to the 7th American Joint Committee on Cancer (AJCC) TNM Staging for Liver and Intrahepatic Bile Duct Malignancies. Overall survival (OS) was defined as the time from the date of surgery to the date of death without regarding the cause of death, while disease-free survival (DFS) was defined as the time from the date of surgery to the time of disease progression (recurrence, distal metastasis, death). Evaluation of $CD8^+$ T-cell infiltration in histological slides of each patient included in the study was conducted by using the immunochemistry method (electronic supplementary Methods).

Computed Tomography Image Acquisition

The radiomic workflow is presented in Fig. 1. All CT examinations were performed using a 128-row multidetector CT scanner (Somatom Definition Flash; Siemens Medical Systems, Erlangen, Germany). The acquisition protocols are shown in electronic supplementary Table 1. For each patient in our study, a noniodine contrast media of 1.5 mL/kg (300 mg/mL iomeprol; Iomeron, Bracco Altana Pharma, Milan, Italy) was injected intravenously using a power injector at a rate of 2.5 mL/s, followed by a saline

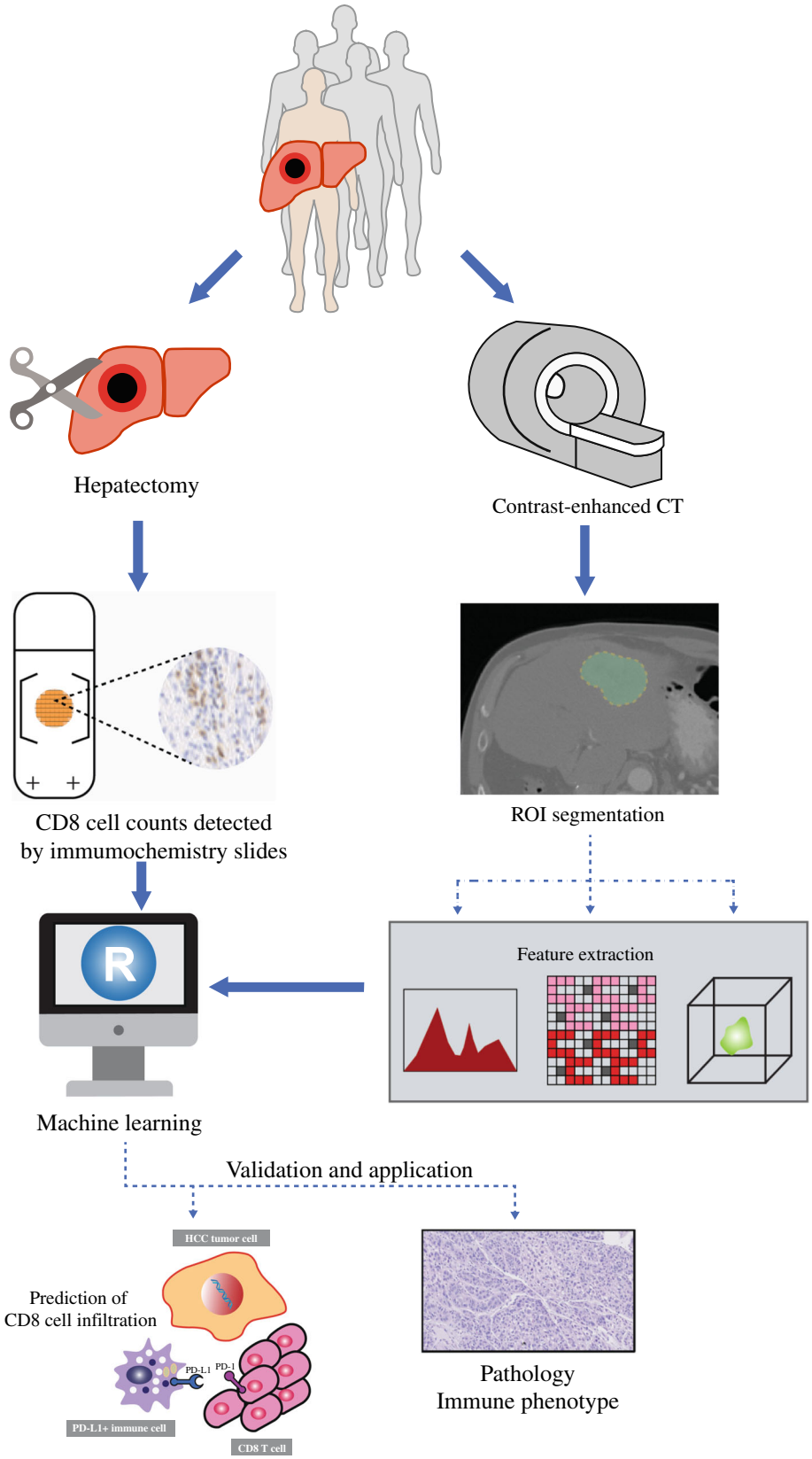

FIG. 1 Radiomic workflow. *ROI* region of interest, *CT* computed tomography

flush (20 mL). During the examination, images from a three-phase scan were obtained, including the pre-contrast phase (30–40 s after injection of the contrast agent), arterial phase (AP; 60–70 s after injection of the contrast agent), and the portal vein phase (PVP; 180 s after injection of the contrast agent). AP CT images were retrieved for image feature extraction.

Tumor Segmentation

Three-dimensional segmentation of tumor regions of interest (ROIs) was manually performed using ITK-SNAP software (http://www.itksnap.org), which was based on consensus reached by two radiologists with over 10 years of work experience. To capture ROIs, a peripheral ring was created slightly along the visible border of the lesion in all AP images for each patient[17] to include approximately the entire volume of the lesion (Fig. 1). For those cases with a blurred edge around the lesion, the maximum range was drawn and was regarded as the border.

Feature Extraction

The extraction of radiomic features was performed using Artificial Intelligence Kit software (A.K. software, GE Healthcare); detailed information regarding the radiomic features can be found in the electronic supplementary material. To verify whether the features extracted by different radiologists were not significantly different, we used intra- and interclass correlation coefficients (ICC) to assess the intra- and interobserver reproducibility of radiomic feature extraction.[18] Initially, 30 CT images of AP were randomly selected for ROI segmentation and feature extraction. The ROI segmentation was performed by two radiologists, both of whom drew contours of the same lesions in these 30 CT images (total number of contours = 30). An ICC $\geq$ 0.75 indicates good consistency of feature extraction.

Statistical Analysis

All statistical tests were performed using R version 3.5.2 (R Foundation for Statistical Computing, Vienna, Austria). The Wilcoxon signed-rank or Kruskal–Wallis tests were used for numerical variables, and Fisher's exact test was used for categorical variables. High or low $CD8^+$ T-cell infiltration was determined by stratifying patients into two groups based on their median value of $CD8^+$ T-cell density. The median value of Rad score in the training cohort was used to cluster patients into high score (greater than the median value) or low score (less than or equal to the median value) groups. The receiver operating characteristic (ROC) curves were plotted using the 'pROC' package. Decision curve analysis (DCA) was used to evaluate the clinical utility of the Rad score, which was performed using the 'rmda' package. Survival rates of expression level (Rad score high vs. low) were estimated using the Kaplan–Meier method with Rothman's confidence intervals (CIs). Survival curves were compared using the log-rank test and plotted using the 'survminer' package. A two-sided p value < 0.05 was considered statistically significant.

RESULTS

Patient Characteristics

The basic characteristics of patients included in this study are listed in Table 1. Among the 142 patients, 114 (80.3%) were male and the median age was 46 years (interquartile range [IQR] 33.3–63.8). No significant differences in sex, age, HBsAg level, AFP level, TNM stage, differentiation grade, and liver cirrhosis status were observed between the training and validation groups.

TABLE 1 Patient characteristics

	Training group	Validation group	p value
Overall	100	42	
Sex			
Male	79	35	0.7179
Female	21	7	
Age, years			
< 65	81	38	0.2146
≥ 65	19	4	
HbsAg			
Negative	14	3	0.3957
Positive	86	39	
AFP, ng/mL			
< 400	61	24	0.81
≥ 400	39	18	
TNM			
I	49	18	0.7233
II	27	14	
III–IV	24	10	
ES grade			
I–II	5	0	0.472
III	51	23	
IV	44	19	
Liver cirrhosis			
No	33	21	0.08632
Yes	67	21	

HbsAg surface antigen of the hepatitis B virus, *AFP* α-fetoprotein, *ES grade* Edmondson and Steiner grading system

Regarding CD8$^+$ T-cell infiltration, median density in the training and validation groups was 6.92/mm^3 (IQR 2.96–18.97) and 6.323/mm^3 (3.07–12.1), respectively (Student's t test $p = 0.89$).

Radiomic Score Construction

The study flowchart is presented in Fig. 2. By using A.K. software, a total of 385 imaging features were extracted from each AP CT image, including 42 histogram parameters, 36 texture parameters, 9 form factor parameters, 118 grey level co-occurrence matrix (GLCM) parameters, and 180 grey level run-length matrix (GLRLM) parameters. All extracted features are in agreement with the Image Biomarker Standardization Initiative (IBSI) manual, aiming at radiomics studies.[19] Moreover, favorable intra- and interobserver feature extraction reproducibility was proved by intraobserver and interobserver ICCs ranging from 0.802 to 0.952 and 0.769 to 0.914, respectively. During data processing of the radiomic features, 316 and 22 features were excluded using the minimum inhibitory concentration test and interfeature correlation, respectively (electronic supplementary Fig. S2). Finally, 47 features were included for machine learning. The Rad score was developed using the elastic-net model ($\alpha = 0.5$, log (λ) = 3.32) and retained 7 of 47 features (Fig. 2 and electronic supplementary Fig. S3). The formula for the Rad score calculation is presented in the electronic supplementary Methods, in which the seven selected features can be found. Details of radiomic feature

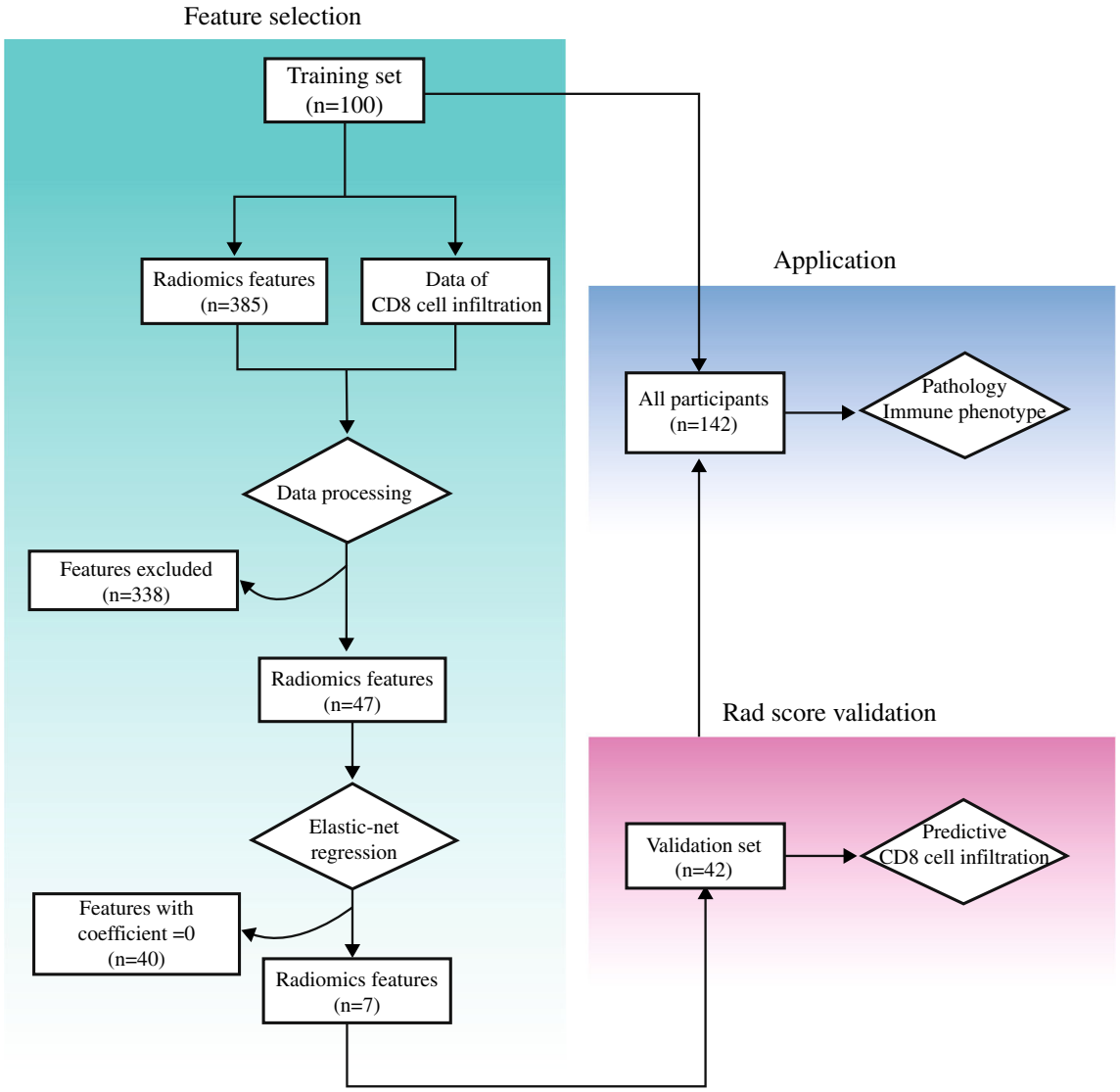

FIG. 2 Study flowchart

selection and radiomic score (Rad score) construction can also be found in the electronic supplementary Methods.

Prediction of CD8$^+$ T-Cell Infiltration by Radiomic Score

According to the median value of CD8$^+$ T-cell density in all patients included in this study (6.80/mm^3), patients were divided into either the CD8-low cohort ($\leq$ 6.80/mm^3, n = 71) or the CD8-high cohort ($>$ 6.80/mm^3, n = 71). In the training set, a significant difference was observed between Rad scores of the CD8-low and CD8-high cohorts (Fig. 3a, left panel; $p < 0.0001$), which was further confirmed in the validation set (Fig. 3b, left panel; $p = 0.0327$). Although Spearman's rhos were only 0.376 and 0.339 in the training and validation cohorts, respectively, there was a statistically significant correlation between CD8$^+$ T-cell infiltration and Rad score when both of these two parameters were viewed as continuous variables in the training (Fig. 3a, right panel; $p = 0.00013$) and validation cohorts (Fig. 3b, right panel; $p = 0.0283$). Moreover, the ability of the radiomic signature to classify high versus low abundance of CD8 infiltration was shown to have an area under the curve (AUC) of 0.751 (95% CI 0.656–0.846) in the training set (Fig. 3c). Further validation on the ability of the Rad score to predict the density of CD8$^+$ T-cell infiltration (Fig. 3d) demonstrated an AUC of 0.705 (95% CI 0.547–0.863). Meanwhile, the DCA curve for the Rad score is presented in Fig. 4, which shows that for the threshold probability within a range of 0–0.91, the Rad score has a higher net benefit than both 'treat all' or 'treat none' strategies.

Previous studies have reported that infiltrating CD8$^+$ T cells in HCC tumor tissues were significantly associated with a low rate of recurrence and prolonged OS.[20–22] Based on the hypothesis that the Rad score could reflect the extent of CD8$^+$ T-cell infiltration, we used the Rad score to predict the OS and DFS outcomes of HCC patients who underwent hepatectomy. The results showed that the OS and DFS rates of patients with higher Rad scores (defined from the training cohort, n = 73) were significantly increased compared with patients with lower Rad scores

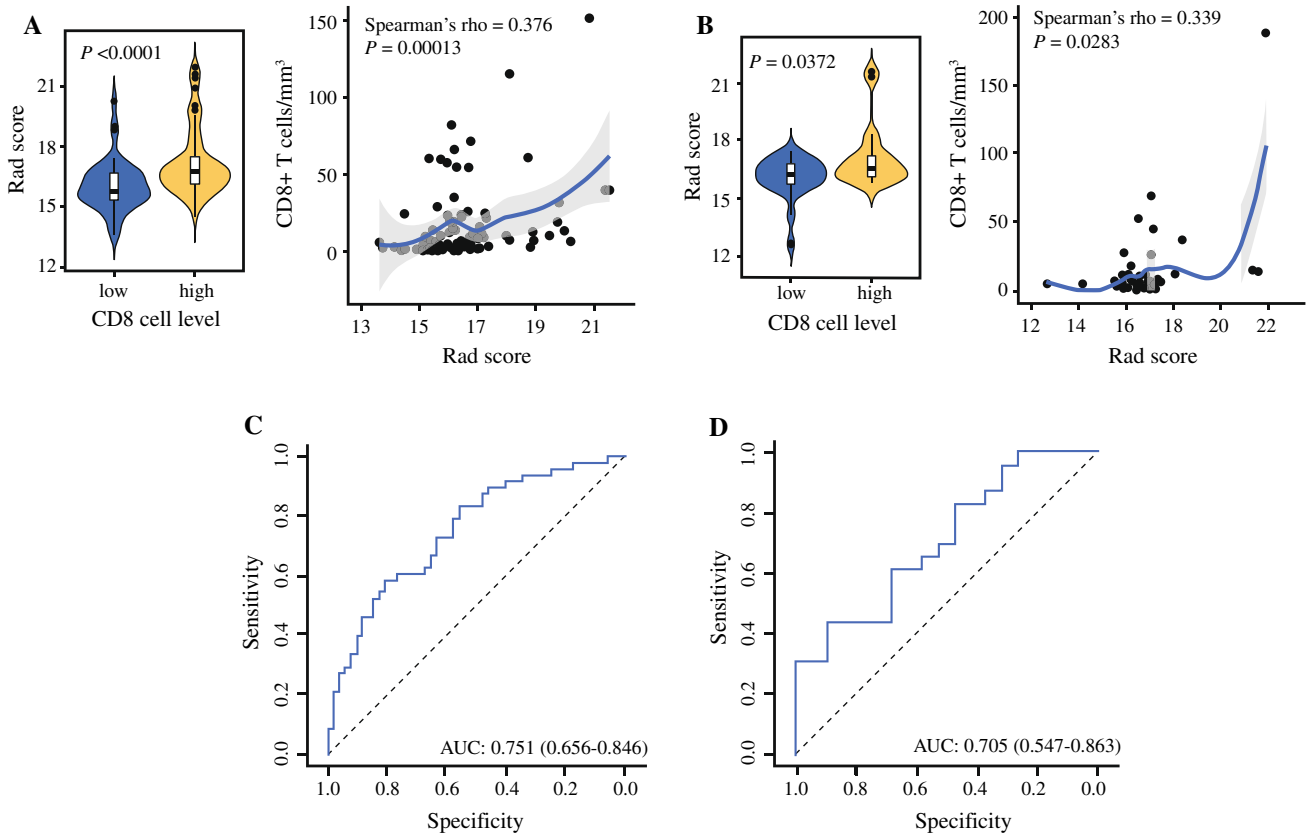

FIG. 3 Performance of the Rad score in the training and validation sets. **a**, **b** Violin plot shows Rad score distributions between the HCC subsets stratified by CD8$^+$ T-cell infiltration in the **a** training and **b** validation cohorts (low vs. high, Mann–Whitney; left panel); scatter plot shows the correlation (Spearman rank; right panel) between the Rad score and CD8$^+$ T-cell infiltration in the **a** training cohort and **b** validation cohort. Blue lines represent LOWESS smoothed fit curve with 95% confidence interval. **c**, **d** AUC of the receiver operator characteristic of Rad scores in the **c** training and **d** validation sets. *AUC* area under the curve, *HCC* hepatocellular carcinoma, *LOWESS* locally weighted scatterplot smoothing

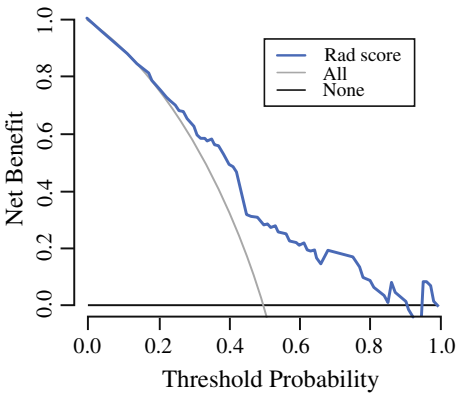

FIG. 4 Decision curve analysis for the Rad score showed that within the threshold probability of between 0 and 0.91, using the Rad score to predict CD8$^+$ T-cell infiltration adds more benefit than treating either all or no patients

(n = 69) (Fig. 5a, b), suggesting an excellent consistency between Rad score and CD8$^+$ T-cell infiltration in predicting the prognosis of HCC patients.

Correlation Between Radiomic Score and Pathological Immune Characteristics

Evidence has been provided that CD8$^+$ T cells comprise the majority of tumor-infiltrating lymphocytes (TILs) in HCC;[23] therefore, we assessed the association between Rad score and the histology of TILs. It was found that the pathologist's quantification of TIL density and Rad score were significantly correlated (Fig. 6a), which in turn validated the strong correlation between CD8$^+$ T-cell infiltration and the abundance of TILs in HCC tissues.

Histologically, three primary immune phenotypes describing the level of CD8$^+$ T-cell presence and activity within the TME, including immune-desert, immune-excluded and inflamed, have been identified and can help determine disruptions or mechanisms of immune escape in cancer immunity.[24] By using the pathology slides of the included HCC patients, we were able to classify each individual by their immune phenotypes. A detailed illustration of these three immune phenotypes can be found in electronic supplementary Fig. S4. Intriguingly, the majority of patients were in the 'immune desert' status (n = 120), while only a small proportion of patients were in the 'immune excluded' status (n = 14) or 'inflamed' status (n = 8). Moreover, our findings showed that the radiomic predictor could significantly discriminate different immune phenotypes on the basis of Rad scores (Fig. 6b).

Conventionally, immunohistochemical expression of PD-1/PD-L1 can serve as a predictor of clinical response to anti-PD-1/PD-L1 immunotherapies in various malignancies.[25,26] In view of the fact that patients with an immunogenic TME of inflamed phenotype had a better clinical response to anti-PD-1/PD-L1 immunotherapies,[10] we evaluated Rad scores in HCC tumors with different PD-L1 or PD-1 expression patterns. As shown in Fig. 6c, d, the Rad scores were significantly higher in tumors with IC-PD-L1$^+$ (n = 21) or TC-PD-L1$^+$ (n = 19) status compared with those with IC-PD-L1$^-$ (Fig. 6c, n = 121) or TC-PD-L1$^-$ (Fig. 6d, n = 123) tumors, respectively. Meanwhile, compared with IC-PD-1$^-$ tumors (n = 114), higher Rad scores could also be found in tumors with IC-PD-1$^+$ status (Fig. 6e, n = 28), which demonstrated the consistency between PD-1 and PD-L1 expressions.[26]

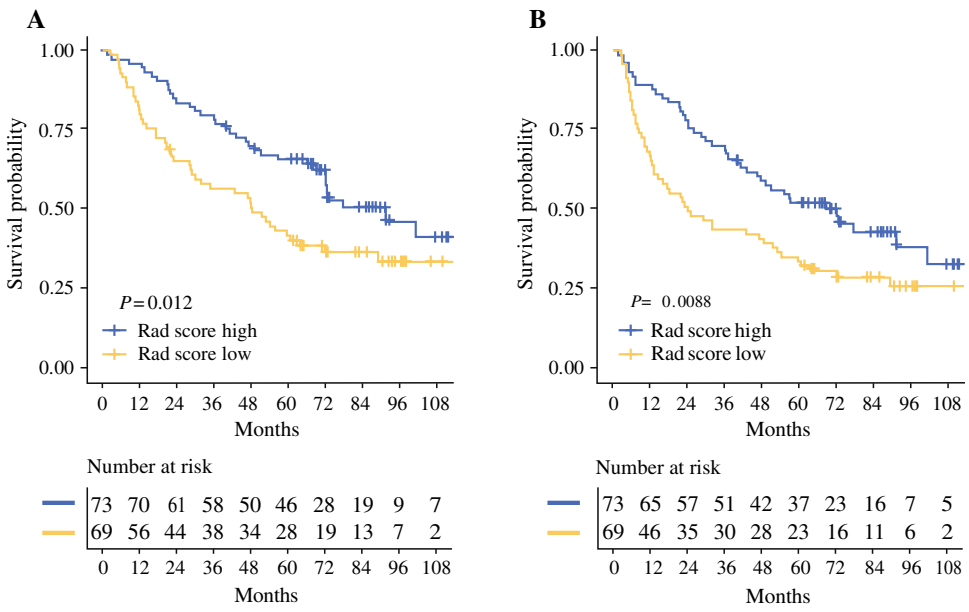

FIG. 5 **a** Overall and **b** disease-free survival of patients relative to the Rad score (high vs. low, as defned by the median value in the training cohort)

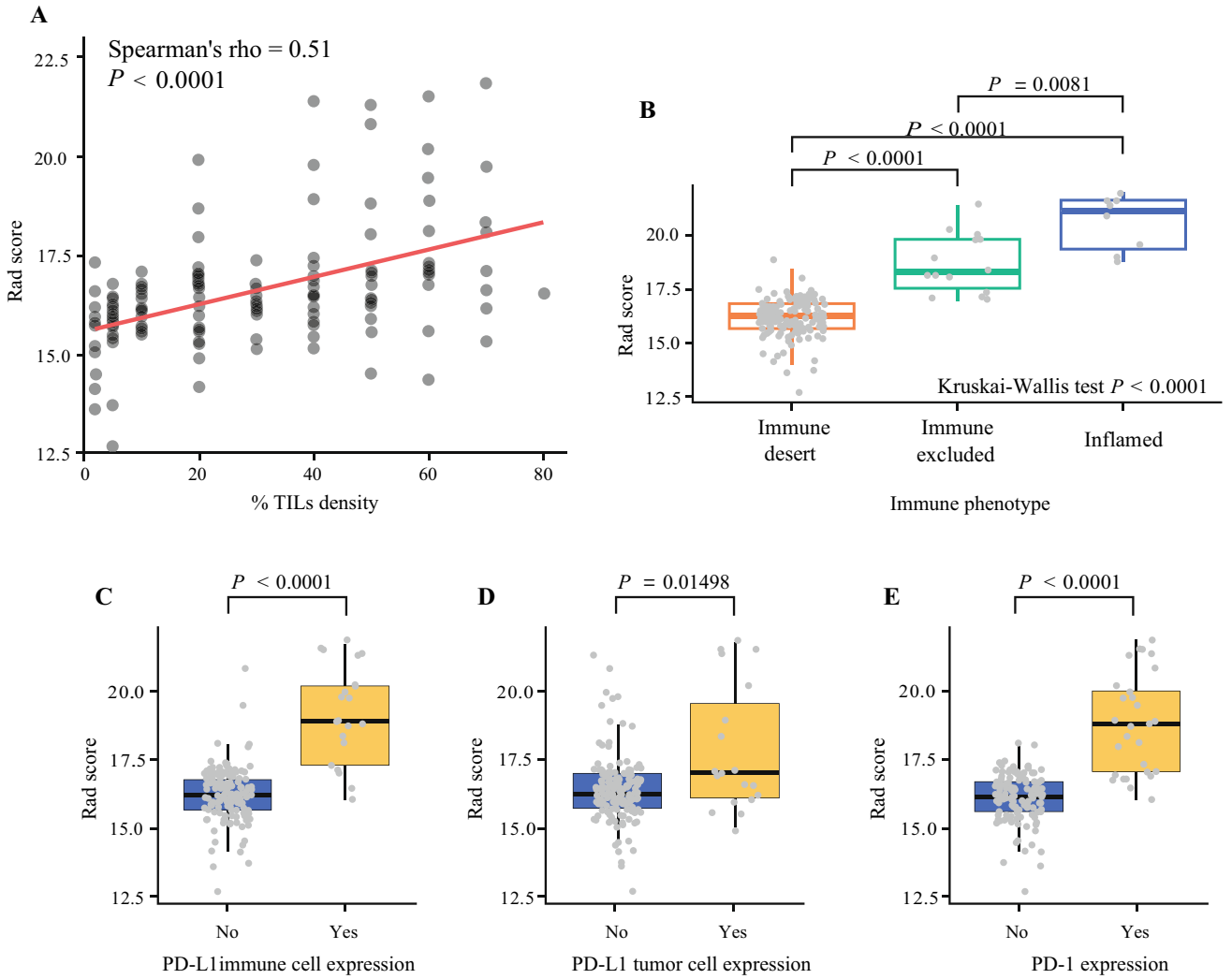

FIG. 6 Evaluation of agreement between the Rad score of $CD8^+$ T cells and pathology. **a** Rad score of $CD8^+$ T cells serves as a predictor of the pathologist's semi-quantification of TILs. **b** Rad score of different immune phenotypes. **c** Rad score distribution between IC-PD-$L1^-$ tumors and IC-PD-$L1^+$ tumors. **d** Rad score distribution between TC-PD-$L1^-$ tumors and TC-PD-$L1^+$ tumors. **e** Rad score distribution between IC-PD-1^- tumors and IC-PD-1^+ tumors. *TILs* tumor-infiltrating lymphocytes, *IC-PD-L1* programmed death-ligand 1 expression on immune cells, *TC-PD-L1* programmed death-ligand 1 expression on tumor cells, *PD-1* programmed death-1

DISCUSSION

Owing to the increasing use of immunotherapy in modern clinical practice, understanding the immune status of cancer patients can help physicians identify those who can really benefit from immune therapies. Combined with pathological biopsies, radiomic approaches can help guide the selection of treatment. In this study, we developed a radiomic score to predict $CD8^+$ T-cell infiltration from CT scans of HCC patients. To our knowledge, our study is the first to construct a radiomic algorithm to predict immune infiltration in a large cohort of HCC patients based on contrast-enhanced CT. By assessing the link between imaging features and immune infiltration using the machine learning method, we were able to establish and validate a radiomic algorithm for pretreatment prediction of immune infiltration based on seven imaging features. Moreover, the results also showed the ability of the Rad score to predict survival outcomes, abundance of TILs, immune phenotypes, and PD-1/PD-L1 expression. These facts have strengthened the biological and clinical relevance of the Rad score as a potential biomarker of $CD8^+$ T-cell infiltration in clinical practice.

As shown in the electronic supplementary Methods, our Rad score algorithm consists of parameters from GLRLM and GLCM. According to the reports from Sun et al.,[27] GLRLM parameters could represent inflammatory infiltration, and heterogeneous and intertwined processes, including chaotic vascularization and necrosis in tumors, which intuitively explains the correlation between $CD8^+$

T-cell infiltration and these patterns. On the other hand, GLCM is a rapid mathematical method assessing the structural properties of images, including homogeneity, complexity, and level of disorder.[28] Notably, GLCM entropy parameters, which have been applied in our Rad score algorithm (electronic supplementary Methods), have been proved to be indicators of tissue structural degradation.[29] Considering the high level of structural changes caused by vascularization and necrosis within HCC lesions, this fact has also suggested the association of CD8$^+$ T-cell infiltration with GLCM entropy parameters.

Several clinical studies have demonstrated the prognostic and predictive importance of TILs in various cancer types,[22,30–34] with the notion that a higher abundance of TILs contributed to better survival outcomes. As the most predominant in TILs, the CD8$^+$ T-cell is ascribed the role of cytotoxic killer cell in the context of cancer immunobiology. Thus, infiltration of CD8$^+$ T cells has been regarded as a marker of superior prognosis. Our findings show that not only does a positive correlation exist between the Rad score and TIL infiltration, but also the Rad score can predict both OS and DFS after hepatectomy. Due to the fact that the Rad score acts as a reflection of CD8$^+$ T-cell infiltration, the association between higher Rad scores and better survival can be interpreted, indicating the role of the Rad score as a significant prognosis biomarker for HCC patients.

It has been proved that a major subset of patients with advanced solid tumors shows evidence for an inflamed TME, which is characterized by the presence of TILs, high density of interferon-γ-producing CD8$^+$ T cells, expression of PD-L1 in TILs, possible genomic instability, and the presence of a pre-existing antitumor immune response.[24,35] This phenotype tends to respond to immunotherapy and is positively associated with clinical benefit from treatment.[10,24,36] In immune-excluded tumors, the invasion of CD8$^+$ T cells into tumors was inhibited by several biological signals, including transforming growth factor (TGF)-β signaling, activation of myeloid-derived suppressor cells, and angiogenesis. As for the immune-desert phenotype, no significant CD8$^+$ T-cell infiltration within tumor tissues can be observed by immunohistochemistry (IHC). Both immune-excluded and immune-desert phenotypes were considered to be unresponsive to immunotherapies. Despite the limited number of HCC samples of the inflamed phenotype, the Rad score was able to identify this subgroup of patients who might have a potential response to immunotherapies. On the other hand, the limited number of inflamed HCC tumors in this cohort indicates the point that most HCC patients might not benefit from current immune treatments. Regarding this fact, the clinical value of the Rad score in identifying potential HCC candidates for immunotherapies is of great significance.

The mechanism of responses to anti-PD-1/PD-L1 immunotherapy relieves the inhibition of host immune response (termed adaptive immune resistance) by upregulating PD-L1 and its ligation to PD-1 on antigen-specific CD8$^+$ T cells,[37,38] indicating the hypothesis that both pre-existing CD8$^+$ T-cell and PD-L1 expression might correlate with clinical response to anti-PD-1/PD-L1 immunotherapy. Indeed, this hypothesis has been confirmed by clinical trials across various cancer types.[36] It is notable that PD-L1 can be expressed by both tumor cells and immune cells in HCC tissues, which have different biological and clinical significance.[39,40] Liu and colleagues[40] performed immunohistochemical staining for 453 HCC samples, and demonstrated that IC-PD-L1$^+$ tumors exhibited an activated TME with higher numbers of infiltrating CD8$^+$ T cells compared with IC-PD-L1$^-$ tumors, while no significant difference was observed bewteen TC-PD-L1$^+$ and TC-PD-L1$^-$ tumors. In current study, both TC-PD-L1$^+$ and IC-PD-L1$^+$ tumors exhibited higher Rad scores. Considering the higher proportion of samples co-expressing TC-PD-L1 and IC-PD-L1 in either TC-PD-L1$^+$ or IC-PD-L1$^+$ samples,[40] this finding suggests that Rad score has a higher sensitivity in detecting PD-L1 expression, providing a novel method to select patients for anti-PD-1/PD-L1 therapies when combined with IHC results.

CONCLUSIONS

The Rad score we constructed is an efficient, non-invasive, cost-effective tool to predict immune infiltration in HCC patients, which has promoted the development of non-invasive biomarkers in immunotherapy. Further clinical trials will be inspired to validate our findings in large-scale prospective cohorts.

AUTHOR CONTRIBUTIONS BS and YZ designed the whole project and participated in result evaluation. HL, ML, and ZZ collected the clinical data of HCC candidates. ZZ and JC participated in ROI segmentation and image feature extractions. LX and ZW participated in performing IHC and pathological analysis. HL and ZZ performed image feature selection and radiomic model construction. HL and ZZ conducted the data analysis and wrote the manuscript. KY modified the structure of manuscript. All authors reviewed the manuscript and approved the final version.

FUNDING This work was supported by Grants from the Natural Science Foundation of China (81872004, 81800564, 81770615, 81700555, 81672882 and 81502441), the Science and Technology Support Program of Sichuan Province (2017SZ0003, 2018SZ0115), and the Science and Technology Program of Tibet Autonomous Region (XZ201801-GB-02).

DISCLOSURES Haotian Liao, Zhen Zhang, Jie Chen, Mingheng Liao, Lin Xu, Zhenru Wu, Kefei Yuan, Bin Song, and Yong Zeng declare no competing interests in this work.

REFERENCES

1. Chen W, Zheng R, Baade PD, Zhang S, Zeng H, Bray F, et al. Cancer statistics in China, 2015. *CA Cancer J Clin*. 2016;66(2):115–32.
2. Dhir M, Melin AA, Douaiher J, Lin C, Zhen WK, Hussain SM, et al. A review and update of treatment options and controversies in the management of hepatocellular carcinoma. *Ann Surg*. 2016;263(6):1112–25.
3. European Association for the Study of the Liver. EASL clinical practice guidelines: management of hepatocellular carcinoma. *J Hepatol*. 2018;69(1):182–236.
4. Reck M, Rodriguez-Abreu D, Robinson AG, Hui R, Csoszi T, Fulop A, et al. Pembrolizumab versus chemotherapy for PD-L1-positive non-small-cell lung cancer. *N Engl J Med.* 2016;375(19):1823–33.
5. Robert C, Schachter J, Long GV, Arance A, Grob JJ, Mortier L, et al. Pembrolizumab versus ipilimumab in advanced melanoma. *N Engl J Med*. 2015;372(26):2521–32.
6. Rossi C, Gilhodes J, Maerevoet M, Herbaux C, Morschhauser F, Brice P, et al. Efficacy of chemotherapy or chemo-anti-PD-1 combination after failed anti-PD-1 therapy for relapsed and refractory Hodgkin lymphoma: a series from Lysa centers. *Am J Hematol*. 2018. https://doi.org/10.1002/ajh.25154.
7. Sangro B, Gomez-Martin C, de la Mata M, Inarrairaegui M, Garralda E, Barrera P, et al. A clinical trial of CTLA-4 blockade with tremelimumab in patients with hepatocellular carcinoma and chronic hepatitis C. *J Hepatol*. 2013;59(1):81–8.
8. El-Khoueiry AB, Sangro B, Yau T, Crocenzi TS, Kudo M, Hsu C, et al. Nivolumab in patients with advanced hepatocellular carcinoma (CheckMate 040): an open-label, non-comparative, phase 1/2 dose escalation and expansion trial. *Lancet.* 2017;389(10088):2492–502.
9. Chen DS, Mellman I. Elements of cancer immunity and the cancer-immune set point. *Nature*. 2017;541(7637):321–30.
10. Herbst RS, Soria JC, Kowanetz M, Fine GD, Hamid O, Gordon MS, et al. Predictive correlates of response to the anti-PD-L1 antibody MPDL3280A in cancer patients. *Nature.* 2014;515(7528):563–7.
11. Hugo W, Zaretsky JM, Sun L, Song C, Moreno BH, Hu-Lieskovan S, et al. Genomic and transcriptomic features of response to anti-PD-1 therapy in metastatic melanoma. *Cell.* 2016;165(1):35–44.
12. Kim JM, Chen DS. Immune escape to PD-L1/PD-1 blockade: seven steps to success (or failure). *Ann Oncol.* 2016;27(8):1492–504.
13. Gillies RJ, Kinahan PE, Hricak H. Radiomics: images are more than pictures, they are data. *Radiology*. 2016;278(2):563–77.
14. Lambin P, Rios-Velazquez E, Leijenaar R, Carvalho S, van Stiphout RG, Granton P, et al. Radiomics: extracting more information from medical images using advanced feature analysis. *Eur J Cancer*. 2012;48(4):441–6.
15. Limkin EJ, Sun R, Dercle L, Zacharaki EI, Robert C, Reuze S, et al. Promises and challenges for the implementation of computational medical imaging (radiomics) in oncology. *Ann Oncol*. 2017;28(6):1191–206.
16. Aerts HJ, Velazquez ER, Leijenaar RT, Parmar C, Grossmann P, Carvalho S, et al. Decoding tumour phenotype by noninvasive imaging using a quantitative radiomics approach. *Nat Commun.* 2014;5:4006.
17. Peng J, Zhang J, Zhang Q, Xu Y, Zhou J, Liu LJD, et al. A radiomics nomogram for preoperative prediction of microvascular invasion risk in hepatitis B virus-related hepatocellular carcinoma. *Diagn Interv Radiol*. 2018;24(3):121–7.
18. McAlinden C, Khadka J, Pesudovs K. Statistical methods for conducting agreement (comparison of clinical tests) and precision (repeatability or reproducibility) studies in optometry and ophthalmology. *Ophthalmic Physiol Opt*. 2011;31(4):330–8.
19. Zwanenburg A, Leger S, Vallières M, Löck S. Image biomarker standardisation initiative—feature definitions. 2016.
20. Brunner SM, Rubner C, Kesselring R, Martin M, Griesshammer E, Ruemmele P, et al. Tumor-infiltrating, interleukin-33-producing effector-memory CD8(+) T cells in resected hepatocellular carcinoma prolong patient survival. *Hepatology*. 2015;61(6):1957–67.
21. Gabrielson A, Wu Y, Wang H, Jiang J, Kallakury B, Gatalica Z, et al. Intratumoral CD3 and CD8 T-cell densities associated with relapse-free survival in HCC. *Cancer Immunol Res*. 2016;4(5):419–30.
22. Sideras K, Biermann K, Verheij J, Takkenberg BR, Mancham S, Hansen BE, et al. PD-L1, Galectin-9 and CD8(+) tumor-infiltrating lymphocytes are associated with survival in hepatocellular carcinoma. *Oncoimmunology*. 2017;6(2):e1273309.
23. Wada Y, Nakashima O, Kutami R, Yamamoto O, Kojiro M. Clinicopathological study on hepatocellular carcinoma with lymphocytic infiltration. *Hepatology* 1998;27(2):407–14.
24. Hegde PS, Karanikas V, Evers S. The where, the when, and the how of immune monitoring for cancer immunotherapies in the era of checkpoint inhibition. *Clin Cancer Res*. 2016;22(8):1865–74.
25. Meng X, Huang Z, Teng F, Xing L, Yu J. Predictive biomarkers in PD-1/PD-L1 checkpoint blockade immunotherapy. *Cancer Treat Rev*. 2015;41(10):868–76.
26. Taube JM, Klein A, Brahmer JR, Xu H, Pan X, Kim JH, et al. Association of PD-1, PD-1 ligands, and other features of the tumor immune microenvironment with response to anti-PD-1 therapy. *Clin Cancer Res*. 2014;20(19):5064–74.
27. Sun R, Limkin EJ, Vakalopoulou M, Dercle L, Champiat S, Han SR, et al. A radiomics approach to assess tumour-infiltrating CD8 cells and response to anti-PD-1 or anti-PD-L1 immunotherapy: an imaging biomarker, retrospective multicohort study. *Lancet Oncol*. 2018;19(9):P1180–91.
28. Pantic I, Pantic S, Paunovic J, Perovic M. Nuclear entropy, angular second moment, variance and texture correlation of thymus cortical and medullar lymphocytes: grey level co-occurrence matrix analysis. *An Acad Bras Cienc*. 2013;85(3):1063–72.
29. Shamir L, Wolkow CA, Goldberg IG. Quantitative measurement of aging using image texture entropy. *Bioinformatics*. 2009;25(23):3060.
30. Denkert C, von Minckwitz G, Darb-Esfahani S, Lederer B, Heppner BI, Weber KE, et al. Tumour-infiltrating lymphocytes and prognosis in different subtypes of breast cancer: a pooled analysis of 3771 patients treated with neoadjuvant therapy. *Lancet Oncol*. 2018;19(1):40–50.
31. Erdag G, Schaefer JT, Smolkin ME, Deacon DH, Shea SM, Dengel LT, et al. Immunotype and immunohistologic characteristics of tumor-infiltrating immune cells are associated with clinical outcome in metastatic melanoma. *Cancer Res*. 2012;72(5):1070–80.
32. Galon J, Costes A, Sanchez-Cabo F, Kirilovsky A, Mlecnik B, Lagorce-Pages C, et al. Type, density, and location of immune cells within human colorectal tumors predict clinical outcome. *Science*. 2006;313(5795):1960–4.
33. Sideras K, Biermann K, Yap K, Mancham S, Boor PPC, Hansen BE, et al. Tumor cell expression of immune inhibitory molecules and tumor-infiltrating lymphocyte count predict cancer-specific

survival in pancreatic and ampullary cancer. *Int J Cancer*. 2017;141(3):572–82.
34. Zhang L, Conejo-Garcia JR, Katsaros D, Gimotty PA, Massobrio M, Regnani G, et al. Intratumoral T cells, recurrence, and survival in epithelial ovarian cancer. *N Engl J Med*. 2003;348(3):203–13.
35. Gajewski TF. The next hurdle in cancer immunotherapy: overcoming the non-T-cell-inflamed tumor microenvironment. *Semin Oncol*. 2015;42(4):663–71.
36. Tumeh PC, Harview CL, Yearley JH, Shintaku IP, Taylor EJ, Robert L, et al. PD-1 blockade induces responses by inhibiting adaptive immune resistance. *Nature*. 2014;515(7528):568–71.
37. Pardoll DM. The blockade of immune checkpoints in cancer immunotherapy. *Nat Rev Cancer*. 2012;12(4):252–64.
38. Spranger S, Spaapen RM, Zha Y, Williams J, Meng Y, Ha TT, et al. Up-regulation of PD-L1, IDO, and T(regs) in the melanoma tumor microenvironment is driven by CD8(+) T cells. *Sci Transl Med*. 2013;5(200):200ra116.
39. Calderaro J, Rousseau B, Amaddeo G, Mercey M, Charpy C, Costentin C, et al. Programmed death ligand 1 expression in hepatocellular carcinoma: relationship with clinical and pathological features. *Hepatology*. 2016;64(6):2038–46.
40. Liu CQ, Xu J, Zhou ZG, Jin LL, Yu XJ, Xiao G, et al. Expression patterns of programmed death ligand 1 correlate with different microenvironments and patient prognosis in hepatocellular carcinoma. *Br J Cancer*. 2018;119(1):80–8.